Microchimica Acta
https://doi.org/10.1007/s00604-018-2970-8

ORIGINAL PAPER

Tungsten disulfide (WS_2) nanosheet-based photoelectrochemical aptasensing of chloramphenicol

Yunlei Zhou[1] · Chengji Sui[1] · Huanshun Yin[1] · Yue Wang[1] · Minghui Wang[1] · Shiyun Ai[1]

Received: 20 June 2018 / Accepted: 18 August 2018

Abstract

A method is described for photoelectrochemical determination of chloramphenicol (CLOA). It is based on the use of (a) aptamers protected with photoactive WS_2 nanosheets, and (b) DNase I-assisted target recycling. The DNA aptamer without label was employed for recognition of CLOA. In the absence of CLOA, the aptamer is adsorbed on the surface of WS_2. This leads to a decrease of photocurrent due to the steric-hindrance effect of aptamer DNA. The adsorption of WS_2 also protects the aptamer from digestion by DNase. In the presence of CLOA, the aptamer will be desorbed from the WS_2 surface due to formation of an aptamer/CLOA conjugate. This results in an increased photocurrent due to a decreased amount of aptamer DNA on the electrode surface. The increase of photocurrent can be further improved by applying DNase triggered catalytic recycling of CLOA. Under optimal experimental conditions, the response is linear 10 pM – 10 nM CLOA concentration range, with a 3.6 pM lower detection limit (at 3σ). This method is acceptably selective, accurate and stable. It was applied to the determination of CLOA in spiked milk samples and gave satisfactory results.

Keywords Photoelectrochemistry · Amperometry · Transition metal dichalcogenide · Tungsten disulfide · Antibiotic detection · DNA aptamer · Food sample · Signal amplification

Introduction

Chloramphenicol (CLOA) has been widely used to cure bacterial infections. The overdose intake of CLOA can result in serious side effects, such as bone marrow suppression, kidney damage and allergic reactions [1]. Thus it is crucial to develop various methods for simple, rapid and sensitive detection of CLOA. Up to now, various methods have been employed to detect CLOA, including fluorescence [2], high-performance liquid chromatography with tandem mass spectrometry (HPLC-MS/MS) [3], electrochemistry [4], electrochemiluminescence (ECL) [5] and photoelectrochemical (PEC) method [6].

Among these methods, PEC-based detection is a new platform for bioassay, in which the light is employed to excite the photoactive material to generate electron, then the electron can be transferred to electrode to produce photocurrent as detection signal [7]. Due to the advantages of fast response, simple operation, inexpensive instrument, low background current and low consumption, PEC technique has attracted increasing attentions, and various target can be detected by this technique, such as organic small molecules [8, 9], heavy metal ions [10, 11], nucleic acids and their derivatives [12, 13], proteins [14–16] and cell [17]. In PEC bioassay, photoactive materials are usually designed as the matrix to immobilize or capture the subsequent biological recognition unit. As a kind of two-dimensional inorganic semiconductor nanomaterials with some unusual physical, chemical or electronic properties [18], transition metal dichalcogenides (TMDs) receive more attentions on the field of opto-electronic/electronic devices, electrocatalysis, sensors and energy storage. Among them, WS_2 is promising photoactive nanomaterial in the construction of PEC biosensors [19]. More importantly, WS_2 presents excellent adsorption ability for single-stranded DNA (ssDNA) and fluorescence quenching ability for the labeled dye at the terminal of ssDNA. When ssDNA hybridizes with its

Electronic supplementary material The online version of this article (https://doi.org/10.1007/s00604-018-2970-8) contains supplementary material, which is available to authorized users.

✉ Huanshun Yin
yinhs@sdau.edu.cn

[1] College of Chemistry and Material Science, Shandong Agricultural University, 271018 Taian, Shandong, People's Republic of China

Published online: 12 September 2018

complementary DNA to form double-stranded DNA, or ssDNA interacts with its target molecule to form aptamer-target conjugate, the adsorbed ssDNA can be released from WS_2 surface [20]. Based on this property, WS_2-based nanomaterials have been widely applied in biosensors using fluorescence and electrochemical techniques [21, 22].

Inspired by the excellent properties of WS_2 nanomaterial, a sensitive PEC method was designed with combining the adsorption property and photoactivity of WS_2. As shown in Scheme 1, DNA aptamer was used as CLOA recognition element. After DNA was adsorbed on WS_2 modified ITO electrode (WS_2/ITO) surface, the PEC response of WS_2 was decreased greatly due to hindrance effect of the aptamer DNA, which blocked the transfer of the photogenerated electron of WS_2, and promoted the recombination of photogenerated electron and hole. Moreover, when DNA aptamer was adsorbed on the WS_2 surface, it can protect DNA aptamer to avoid the digestion of DNase I. However, When CLOA was further introduced on electrode surface, CLOA-DNA complex was formed and then released from WS_2 surface, which would lead to the increase of the PEC response due to the decreased hindrance effect. Afterwards, the released DNA was further digested by DNase I, and the CLOA-DNA structure was destroyed, which made the regeneration of CLOA target. The released CLOA then binds to another aptamer, and starts a new cycle. This results in the successive release of aptamer from WS_2 surface. As a result, a small amount of target CLOA can effectively induce the release of lots of DNA aptamer form WS_2/ITO electrode surface, which can lead to the greatly increase the photocurrent. By monitoring the change of photocurrent, the quantitative determination of CLOA can be achieved.

Experimental section

Reagents and instruments

CLOA, florfenicol, thiamphenicol, tobramycin, streptomycin, tetracycline, kanamycin, oxytetracycline, ampicillin, amoxicillin, penicillin, lincomycin, melamine, tris(hydroxymethyl)aminomethane (Tris), EDTA, $MgCl_2$,, $CaCl_2$ and KCl were provided by Aladdin (Shanghai, China, http://www.aladdin-e.com/). DNase I was provided by New England Biolab (USA, http://www.neb-china.com/). WS_2 was purchased Sigma (USA, https://www.sigmaaldrich.com). DNA was offered by Sangon Biotech. (Shanghai, China, https://www.sangon.com/). The sequences were as follows. DNA aptamer, 5′-AGC AGC ACA GAG GTC AGA TGC ACT CGG ACC CCA TTC TCC TTC CAT CCC TCA TCC GTC CAC CCT ATG CGT GCT ACC GTG AA-3′. ITO conductive glass was purchased from Zhuhai Kaivo Electronic Components Co., Ltd. (Zhuhai, China, ITO coating 180 ± 25 nm, sheet resistance <15 Ω/cm^2, http://www.zh-kv.com).

The buffers used in this work were as follows. DNA dissolution buffer, 10 mM Tris-HCl and 1 mM EDTA, pH 8.0. DNase I buffer, 10 mM Tris-HCl (pH 7.6), 2.5 mM $MgCl_2$, 0.5 mM $CaCl_2$. Washing buffer, 10 mM Tris-HCl and 50 mM KCl, pH 7.4. Detection buffer, 10 mM Tris-HCl, pH 7.4.

The X-ray diffraction patterns were recorded using a D8 advance (Bruker-AXS, Germany) diffractometer with Cu K_a radiation ($\lambda = 0.1546$ nm). The morphologies and structures of WS_2 were characterized by scanning electron microscopy (SEM, FEI-QUANTA400, USA) and transmission electron microscopy (TEM, Tecnai G2 F20 S-TWIN, FEI, USA). The Raman spectroscopy was performed using a Raman

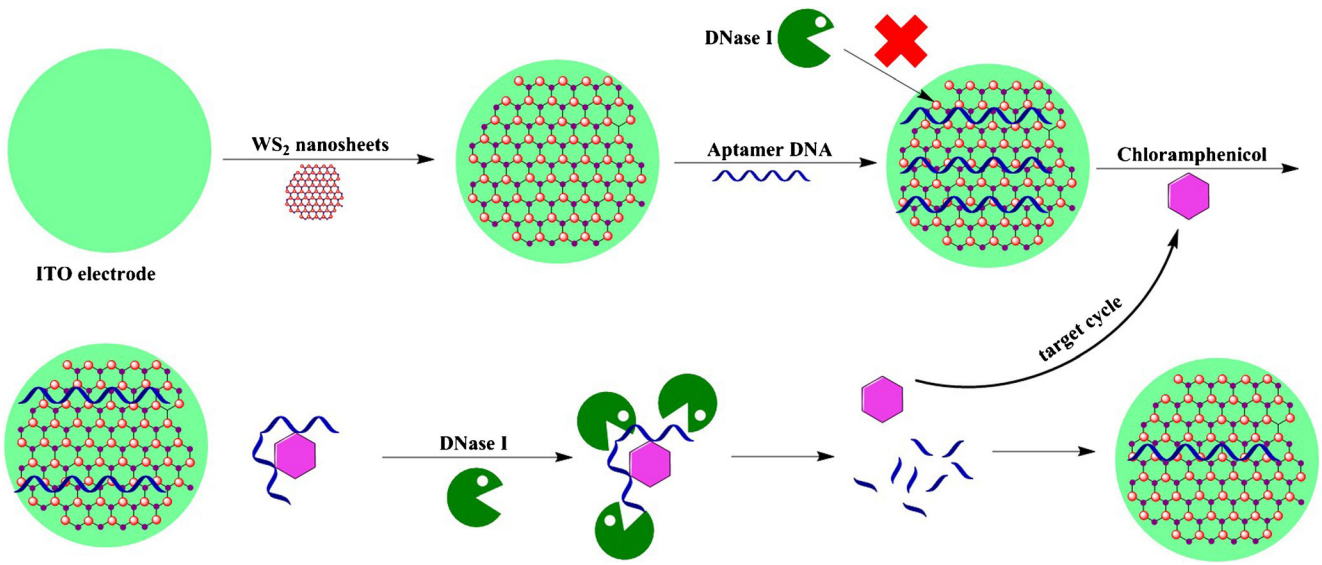

Scheme 1 Schematic representation of the PEC assay strategy and CLOA detection

spectrometer (Horiba XploRA™ PLUS, France) with laser excitation at 638 nm.

Electrode fabrication

Firstly, the ITO conductive glass was first cut into 5.0 × 1.0 cm^2 pieces and sonicated respectively in ethanol/NaOH mixed solution (*v*/v, 1:1), acetone and double distilled deionized water for 30 min, followed by drying at 60 °C for 2 h. Then, 12 mg WS_2 was dispersed into 4 mL water and sonicated for 30 min to obtain a well dispersion solution with the concentration of 3 mg mL^{-1}. After that, 40 μL WS_2 dispersion solution was dropped on ITO electrode surface and dried under infrared lamp irradiation. The prepared electrode was noted as WS_2/ITO. After the electrode was rinsed with washing buffer and dried under N_2 blowing, 20 μL of 5 μM aptamer DNA was dripped onto the electrode surface and incubated for 60 min at room temperature in a humid cell. The electrode was then washed with washing buffer and dried under N_2 blowing. The electrode was marked as DNA/WS_2/ITO. Afterwards, the electrode was further incubated with 20 μL of mixed solution containing various concentrations of target CLOA and 50 unit mL^{-1} DNase I for 105 min at 37 °C under humid conditions. Finally, the electrode was washed with washing buffer and dried under N_2 blowing.

Photoelectrochemical (PEC) detection

PEC experiments were performed on a home-built PEC system. A 500 W Xe lamp equipped with optical filter is used as the irradiation source to produce the visible-light (Light intensity is 20 mW/cm^2). The photocurrent is recorded on a CHI832A electrochemical workstation (CH instruments, Austin, USA) with a three-electrode system in detection buffer. A modified ITO electrode with an area of 0.195 cm^2 is used as the working electrode, a Pt wire as the counter electrode and an SCE as the reference electrode. The working potential is −0.3 V. In addition, the photocurrent was denoted as I ($I = I_{\text{light on}} - I_{\text{light off}}$), where $I_{\text{light on}}$ was the photocurrent with light irradiation, and $I_{\text{light off}}$ was the photocurrent without light irradiation.

Pretreatment of chicken feed and milk powder samples

The chicken feed sample was purchased from a local market, which was pretreated according to previous report with some revision [23]. In brief, 1.0 g chicken feed was grinded using agate mortar. Then, the powder was added into 10 mL Tris-HCl (pH 7.4) and sonicated for 30 min. The dispersion was centrifuged at 12000 rpm for 30 min and filtrated with 0.22 μm filter membrane. Finally, the filtrate was diluted with Tris-HCl (pH 7.4) to prepare the sample for measurement.

The milk powder sample was purchased from a local supermarket. The sample was treated with previous report with minor revision [24]. In brief, 1.0 g milk powder was added into 10.0 mL 10 mM Tris-HCl (pH 7.4) and stirred for 15 min. Then, the pH of the solution was adjusted to 4.6 by 20% acetic acid. After incubating for 30 min, the sample was centrifuged to remove the coagulation of proteins and fats. Subsequently, the collected solution was filtered with 0.22 μm filter membrane. Finally, the pH solution was adjusted to 7.4 for measurement.

Results and discussion

Choice of materials

Recently, transition metal dichalcogenides (TMDs) receive more and more attentions in many fields due to the advantages of unusual physical, chemical or electronic properties. Especially, TMDs also present the PEC property with visible-light activity, which make them alternative material for PEC assay. In addition, TMDs can adsorb ssDNA, and the adsorbed ssDNA can be released from TMDs surface after hybridization or formation DNA-target conjugate. Based on it, TMDs materials have been widely applied in the field of biosensing. Among various TMDs materials, WS_2 attracts our attentions due to its good visible-light activity, strong PEC response (higher than MoS_2 [25]), low cytotoxicity (lower than MoS_2 and WSe_2, graphene and its analogues [26]), thus WS_2 was employed as photoactive material in this work.

Characterization of WS_2

WS_2 was characterized by SEM, TEM, XRD and Raman spectroscopy. The results are shown in Fig. 1. SEM image indicates that WS_2 contains many WS_2 layers in its structure (Fig. 1a). As shown in Fig. 1b, transport sheets are observed by TEM image. It also illustrates that WS_2 contains layer structure. The XRD pattern of WS_2 was investigated. As illustrated in Fig. 1c, all peaks of pure WS_2 show the characteristics of the hexagonal WS_2 (JCPDS card No. 08–0237). The diffraction peaks at 2θ values of 14.6°, 29.08°, 32.84°, 33.84°, 39.72°, 44.16°, 49.8°, 58.44°, 60.8°, 69.4°, 76.08° and 88.6° are corresponding to (002), (004), (100), (101), (103), (006), (105), (110), (112), (201), (116) and (118) planes of WS_2. As illustrated in Fig. 1d, the Raman spectra exhibited the characteristic bands at 351 and 422 cm^{-1}, corresponding to in plane vibration E^1_{2g} mode and out of plane vibration mode (A^1_g) of WS_2, respectively.

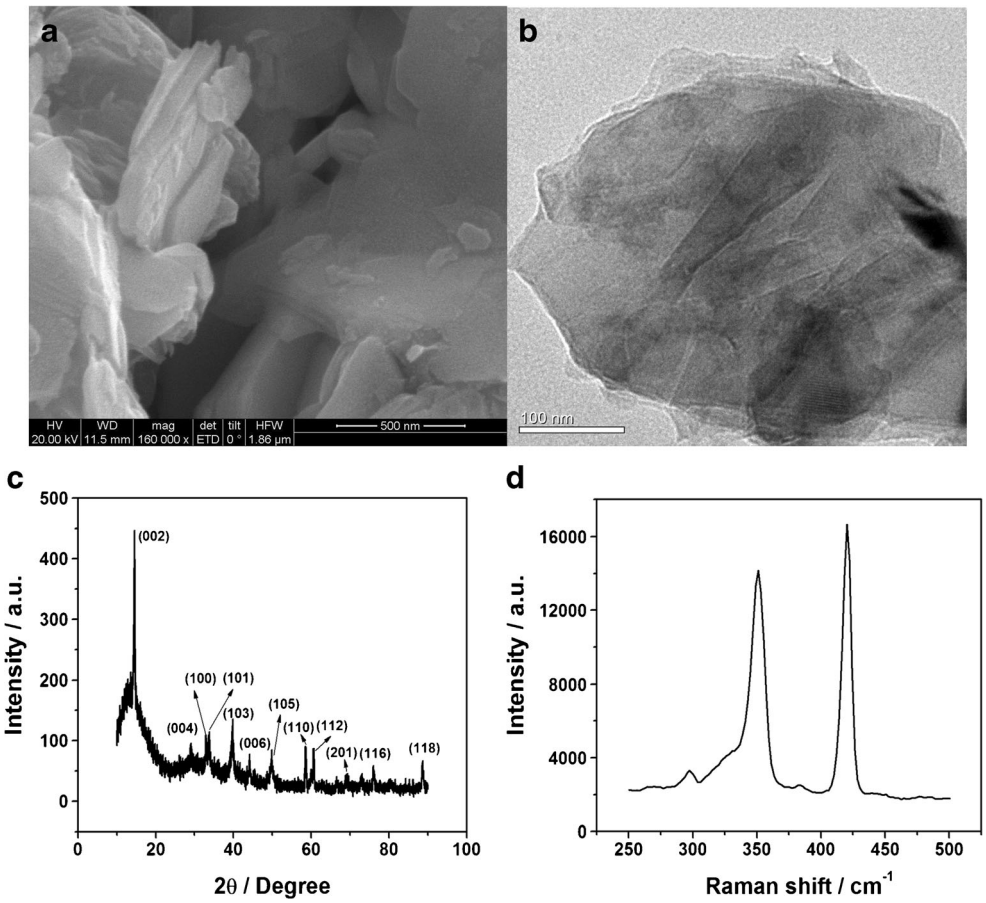

Fig. 1 SEM (**a**) and TEM (**b**) images of WS_2. (**c**) XRD pattern of WS_2. (**d**) Raman spectrum of WS_2

Detection feasibility assay

The detection feasibility of this PEC method was investigated by monitoring the photocurrent change of the ITO electrode with different modification processes. As shown in Fig. 2, the bare ITO electrode presents no PEC response due to the absence of the photoactive material (curve a). Then, a PEC response is observed after WS_2 was modified on ITO electrode surface (curve b), indicating the PEC activity of WS_2. Afterwards, the PEC response is decreased when DNA was adsorbed on electrode surface (curve c), which can be ascribed to the modified aptamer DNA, blocking the transfer of the photogenerated electron and improving the recombination of hole and electron. However, after DNA/WS_2/ITO electrode was incubated with CLOA and DNase I, the photocurrent increased greatly (curve d), which can be explained as the fact that the DNA aptamer was released from electrode surface due to the formation of aptamer-CLOA complex, which further induced DNase I mediated target CLOA recycling. For testifying the signal amplification effect of DNase I, control experiment was performed. As seen in curve e, when the DNA/WS_2/ITO electrode was only incubated with CLOA, the photocurrent still increased, but the increase level was lower than that the electrode was incubated with CLOA and DNase I together, which powerfully demonstrated the important signal amplification effect of DNase I. The above results also prove that this method can be used to detect CLOA.

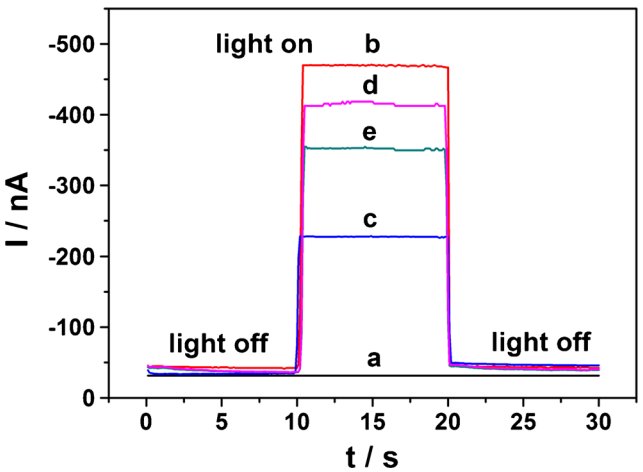

Fig. 2 The PEC response of different electrodes in 10 mM Tris-HCl (pH 7.4). (*a*) ITO, (*b*) WS_2/ITO, (*c*) DNA/WS_2/ITO, (*d*) DNA/WS_2/ITO after incubated with the complex of 1 nM CLOA and 50 unit mL^{-1} DNase I, (*e*) DNA/WS_2/ITO after incubated with 1 nM CLOA

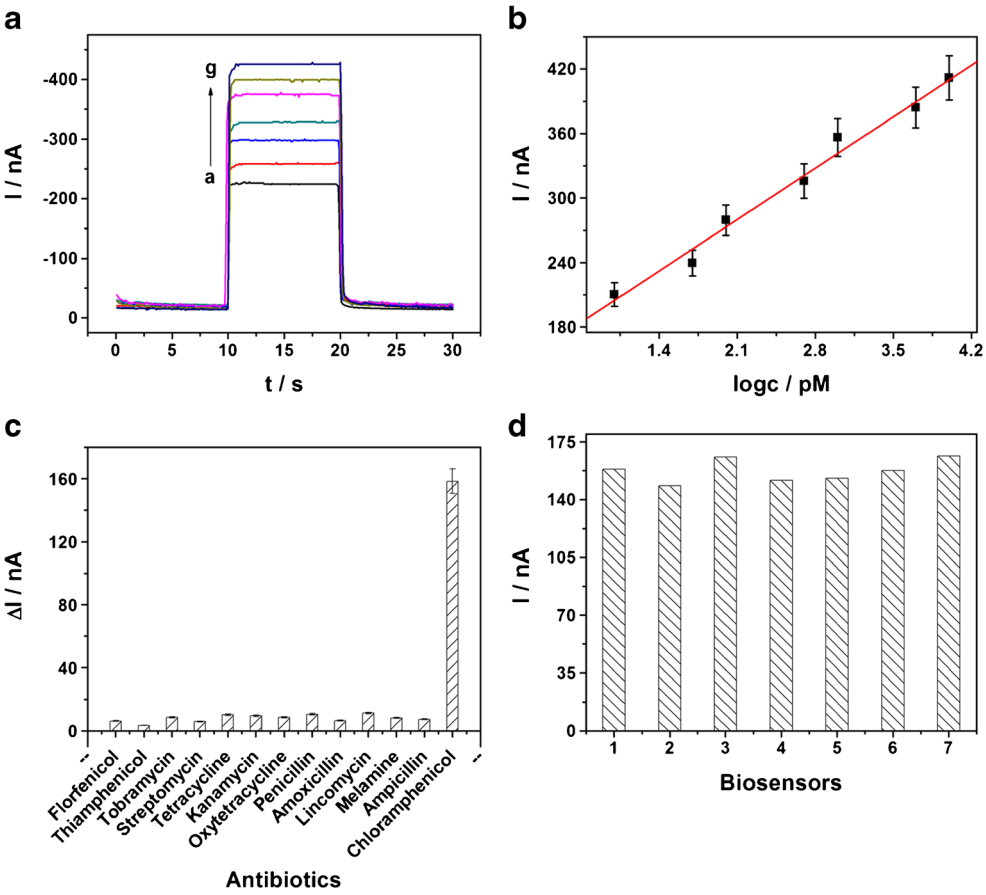

Fig. 3 **a** The PEC response of this method with different concentrations of CLOA under optimal conditions. a-g: 10, 50, 100, 500, 1000, 5000, 10,000 pM. **b** The linear relationship between the photocurrent and the logarithm value of CLOA concentration. **c** The histogram of the photocurrent with different antibiotics. Antibiotic concentration was 1 nM. (D) The histogram of the photoelectrochemical response of seven electrodes with 1 nM CLOA. The photocurrent was recorded in in 10 mM Tris-HCl (pH 7.4)

Optimization of experimental conditions

The following parameters were optimized: (a) WS_2 concentration; (b) aptamer DNA concentration; (c) DNA incubation time; (d) CLOA incubation time. Respective data and Figures are given in the Electronic Supporting Material. In short, the following experimental conditions were found to give best results: (a) Optimal WS_2 concentration:

Table 1 The comparison of the detection performances of the PEC method with other reports on CLOA detection

Methods	Linear range	Detection limit	Refs.
Fluorescence	0.003–10 nM	1 pM	[2]
Fluorescence	0.10–70.00 μM	33 nM	[27]
Colorimetric immunoassay	0.03–12.53 nM	0.03 nM	[28]
Piezoelectric immunosensor	1.55–310 nM	0.62 nM	[29]
Electrochemistry	0.01–1 μM 1–400 μM	2.9 nM	[4]
Electrochemistry	40 pM– 1 μM	17 pM	[30]
Electrochemistry	0.01–35 μM	2 nM	[24]
Capillary zone electrophoresis	–	1.55 μM	[31]
HPLC-MS/MS	0.15 nM – 0.31 μM	–	[3]
Electrochemistry	1.6–420 nM	1.6 nM	[32]
Electrochemiluminescence	0.2–150 nM	70 pM	[5]
Chemiluminescent immunoassay	0.6–10 μM	0.16 μM	[33]
Electrochemistry	1–1000 nM	0.29 nM	[34]
Photoelectrochemistry	10–250 nM	3.1 nM	[6]
Photoelectrochemistry	1.0 pM – .0 nM	0.36 pM	[35]
Photoelectrochemistry	10 pM – 0 nM	3.6 pM	This work

Table 2 Detection CLOA in chicken feed and milk powder samples using the PEC method

Samples	Added	Detected	RSD (%)[a]	Recovery (%)
Chicken feed	10 nM	9.68 nM	4.12	96.8
	1 nM	1.06 nM	4.89	106
	0.1 nM	0.108 nM	7.57	108
Milk powder	10 nM	9.48 nM	3.58	94.8
	1 nM	1.08 nM	5.24	108
	0.1 nM	0.11 nM	8.27	110

[a] The RSD value is calculated for the detected chloramphenicol content for 7 times

3 mg mL^{-1} (b) Optimal aptamer DNA concentration: 5 μM; (c) Optimal DNA incubation time: 60 min; (d) Optimal CLOA incubation time: 105 min.

Detection performances

The detection sensitivity was estimated by detecting different concentrations of CLOA. As shown in Fig. 3a, under optimal experiment conditions, the photocurrent increases gradually with changing CLOA concentration from 10 pM to 10 nM. In the range form 10 pM to 10 nM, the linear relationship between the photocurrent and the logarithm value of CLOA concentration can be achieved The linear regression equation can be expressed as I (nA) = 68.26log$c$ (nM) + 136.9 (R = 0.9914, Fig. 3b). The detection limit was estimated to be 3.6 pM (3σ). The detection performances of this work are compared with other work and the comparison results are listed in Table 1. It indicates that the detection performances of this work are comparable to some of previous work.

The detection specificity of this method was investigated by detecting different antibiotics, such as CLOA, florfenicol, thiamphenicol, tobramycin, streptomycin, tetracycline, kanamycin, oxytetracycline, ampicillin, amoxicillin, penicillin, lincomycin and melamine. The photocurrent change ($\Delta I = I_1 - I_2$) is compared, where I_1 is the photocurrent of DNA/WS_2/ITO after incubated with antibiotics and DNase I, and I_2 is the photocurrent of DNA/WS_2/ITO,. As shown in Fig. 3c, the ΔI for CLOA (1 nM) is greatly higher than that for other antibiotics (1 nM), indicating good detection selectivity.

Detection reproducibility is also a crucial parameter for analysis method. To investigate it, DNA/WS_2/ITO was incubated with 1 nM CLOA and 50 unit mL^{-1} DNase I. Seven electrodes were fabricated with this process independently. The relative standard deviation of the photocurrent is 4.42%, indicating good detection reproducibility (Fig. 3d).

Stability is an important parameter for analytical method, thus it is evaluated. To perform this investigation, DNA/WS_2/ITO was firstly stored at 4 °C in a refrigerator under humid condition for 5 and 10 days, respectively. Then, the electrode was further incubated with 1 nM CLOA and 50 unit mL^{-1} DNase I as described in "Electrode fabrication" section. Finally, the PEC response was recorded and compared. After storage for 5 and 10 days, the PEC method can remain its original photocurrent of 95.15 and 90.34%, indicating acceptable storage stability.

Sample detection

To verify the feasibility and application potential of this PEC method, it was applied to detect CLOA in chicken feed and milk powder samples. After pretreatment, the solution was measured by this PEC method. Because no CLOA was detected in these samples, CLOA standard solutions with different concentrations were added into these samples and the recovery experiments were performed. As shown in Table 2, the recoveries of CLOA from the spiked milk powder samples are ranged from 94.8 to 110%, and the RSDs are ranged from 3.58 to 8.27%.These results also confirm the feasibility of this method for CLOA detection in real samples.

Conclusions

In summary, a selective PEC method was investigated for CLOA detection based on the specific interaction between DNA aptamer and WS_2, and DNase I. Due to the specific recognition of DNA aptamer to CLOA and enzymatic signal amplification, this PEC method showed high detection selectivity and sensitivity. This PEC method was also proved to possess the applicability for detecting CLOA in milk powder samples. More importantly, if only the aptamer was replaced by other antibiotic's aptamer, this method can also be applied to detect other antibiotics. Though this method exist the shortcoming of time-consuming, it still possesses some merits, including simple operation, inexpensive instrument, high sensitivity and high selectivity, which make it attractive method for antibiotic detection.

Acknowledgements This work was supported by the National Natural Science Foundation of China (No.21775090), the Natural Science Foundation of Shandong province, China (No. ZR2016BM10, ZR2018MB028).

Compliance with ethical standards The author(s) declare that they have no competing interests.

References

1. Wang L, Zhang Y, Gao X, Duan Z, Wang S (2010) Determination of chloramphenicol residues in milk by enzyme-liinked immunosorbent assay: improvement by biotin-streptavidin-amplified

system. J Agric Food Chem 58(6):3265–3270. https://doi.org/10.1021/jf903940h
2. Miao Y-B, Ren H-X, Gan N, Cao Y, Li T, Chen Y (2016) Fluorescent aptasensor for chloramphenicol detection using DIL-encapsulated liposome as nanotracer. Biosens Bioelectron 81:454–459. https://doi.org/10.1016/j.bios.2016.03.034
3. Jianbing W, Linyao C, Peipei M, Yanbin L, Huizhong W (2012) Determination of chloramphenicol in aquatic products by graphene-based SPE coupled with HPLC-MS/MS. J Sep Sci 35(24):3586–3592. https://doi.org/10.1002/jssc.201200617
4. Xiao L, Xu R, Yuan Q, Wang F (2017) Highly sensitive electrochemical sensor for chloramphenicol based on MOF derived exfoliated porous carbon. Talanta 167:39–43. https://doi.org/10.1016/j.talanta.2017.01.078
5. Feng X, Gan N, Zhang H, Yan Q, Li T, Cao Y, Hu F, Yu H, Jiang Q (2015) A novel "dual-potential" electrochemiluminescence aptasensor array using CdS quantum dots and luminol-gold nanoparticles as labels for simultaneous detection of malachite green and chloramphenicol. Biosens Bioelectron 74:587–593. https://doi.org/10.1016/j.bios.2015.06.048
6. Liu Y, Yan K, Okoth OK, Zhang J (2015) A label-free photoelectrochemical aptasensor based on nitrogen-doped graphene quantum dots for chloramphenicol determination. Biosens Bioelectron 74:1016–1021. https://doi.org/10.1016/j.bios.2015.07.067
7. Zhao W-W, Xu J-J, Chen H-Y (2015) Photoelectrochemical bioanalysis: the state of the art. Chem Soc Rev 44(3):729–741. https://doi.org/10.1039/c4cs00228h
8. Hun X, Wang S, Wang S, Zhao J, Luo X (2017) A photoelectrochemical sensor for ultrasensitive dopamine detection based on single-layer NanoMoS$_2$ modified gold electrode. Sensors Actuators B Chem 249:83–89. https://doi.org/10.1016/j.snb.2017.04.065
9. Qin C, Bai X, Zhang Y, Gao K (2018) Photoelectrochemical CdSe/TiO$_2$ nanotube array microsensor for high-resolution in-situ detection of dopamine. Microchim Acta 185(5):278. https://doi.org/10.1007/s00604-018-2788-4
10. Wang Y, Wang P, Wu Y, Di J (2018) A cathodic "signal-on" photoelectrochemical sensor for Hg^{2+} detection based on ion-exchange with ZnS quantum dots. Sensors Actuators B Chem 254:910–915. https://doi.org/10.1016/j.snb.2017.07.149
11. Shi Y, Zhang G, Li J, Zhang Y, Yu Y, Wei Q (2017) Photoelectrochemical determination of Hg(II) via dual signal amplification involving SPR enhancement and a folding-based DNA probe. Microchim Acta 184(5):1379–1387. https://doi.org/10.1007/s00604-017-2141-3
12. Yang Z, Shi Y, Liao W, Yin H, Ai S (2016) A novel signal-on photoelectrochemical biosensor for detection of 5-hydroxymethylcytosine based on in situ electron donor producing strategy and all wavelengths of light irradiation. Sensors Actuators B Chem 223:621–625. https://doi.org/10.1016/j.snb.2015.09.159
13. Wang M, Yin H, Zhou Y, Han J, He T, Cui L, Ai S (2018) Photoelectrochemical biosensor for microRNA detection based on multiple amplification strategies. Microchim Acta 185(5):257. https://doi.org/10.1007/s00604-018-2808-4
14. Zhou Q, Lin Y, Shu J, Zhang K, Yu Z, Tang D (2017) Reduced graphene oxide-functionalized FeOOH for signal-on photoelectrochemical sensing of prostate-specific antigen with bioresponsive controlled release system. Biosens Bioelectron 98:15–21. https://doi.org/10.1016/j.bios.2017.06.033
15. Cheng W, Pan J, Yang J, Zheng Z, Lu F, Chen Y, Gao W (2018) A photoelectrochemical aptasensor for thrombin based on the use of carbon quantum dot-sensitized TiO$_2$ and visible-light photoelectrochemical activity. Microchim Acta 185(5):263. https://doi.org/10.1007/s00604-018-2800-z
16. Liu X-P, Xie X-L, Wei Y-P, Mao C-j, Chen J-S, Niu H-L, Song J-M, Jin B-K (2018) Photoelectrochemical immunoassay for human interleukin 6 based on the use of perovskite-type LaFeO$_3$ nanoparticles on fluorine-doped tin oxide glass. Microchim Acta 185(1):52. https://doi.org/10.1007/s00604-017-2554-z
17. Zhang X, Liu M, Liu H, Zhang S (2014) Low-toxic Ag$_2$S quantum dots for photoelectrochemical detection glucose and cancer cells. Biosens Bioelectron 56:307–312. https://doi.org/10.1016/j.bios.2014.01.033
18. Tan C, Zhang H (2015) Two-dimensional transition metal dichalcogenide nanosheet-based composites. Chem Soc Rev 44(9):2713–2731. https://doi.org/10.1039/c4cs00182f
19. Tan Y, Li M, Ye X, Wang Z, Wang Y, Li C (2018) Ionic liquid auxiliary exfoliation of WS$_2$ nanosheets and the enhanced effect of hollow gold nanospheres on their photoelectrochemical sensing towards human epididymis protein 4. Sensors Actuators B Chem 262:982–990. https://doi.org/10.1016/j.snb.2018.02.066
20. Xi Q, Zhou D-M, Kan Y-Y, Ge J, Wu Z-K, Yu R-Q, Jiang J-H (2014) Highly sensitive and selective strategy for microRNA detection based on WS$_2$ nanosheet mediated fluorescence quenching and duplex-specific nuclease signal amplification. Anal Chem 86(3):1361–1365. https://doi.org/10.1021/ac403944c
21. Zuo X, Zhang H, Zhu Q, Wang W, Feng J, Chen X (2016) A dual-color fluorescent biosensing platform based on WS$_2$ nanosheet for detection of Hg^{2+} and ag^{+}. Biosens Bioelectron 85:464–470. https://doi.org/10.1016/j.bios.2016.05.044
22. Zhu C, Zeng Z, Li H, Li F, Fan C, Zhang H (2013) Single-layer MoS$_2$-based nanoprobes for homogeneous detection of biomolecules. JACS 135(16):5998–6001. https://doi.org/10.1021/ja4019572
23. Dechtrirat D, Yingyuad P, Prajongtat P, Chuenchom L, Sriprachuabwong C, Tuantranont A, Tang I-M (2018) A screen-printed carbon electrode modified with gold nanoparticles, poly(3,4-ethylenedioxythiophene), poly(styrene sulfonate) and a molecular imprint for voltammetric determination of nitrofurantoin. Microchim Acta 185(5):261. https://doi.org/10.1007/s00604-018-2797-3
24. Liu S, Lai G, Zhang H, Yu A (2017) Amperometric aptasensing of chloramphenicol at a glassy carbon electrode modified with a nanocomposite consisting of graphene and silver nanoparticles. Microchim Acta 184(5):1445–1451. https://doi.org/10.1007/s00604-017-2138-y
25. Pesci FM, Sokolikova MS, Grotta C, Sherrell PC, Reale F, Sharda K, Ni N, Palczynski P, Mattevi C (2017) MoS$_2$/WS$_2$ heterojunction for photoelectrochemical water oxidation. ACS Catal 7(8):4990–4998. https://doi.org/10.1021/acscatal.7b01517
26. Teo WZ, Chng ELK, Sofer Z, Pumera M (2014) Cytotoxicity of exfoliated transition-metal dichalcogenides (MoS$_2$, WS$_2$, and WSe$_2$) is lower than that of graphene and its analogues. Chem Eur J 20(31):9627–9632. https://doi.org/10.1002/chem.201402680
27. Tan Z, Xu H, Li G, Yang X, Choi MMF (2015) Fluorescence quenching for chloramphenicol detection in milk based on protein-stabilized Au nanoclusters. Spectrochim Acta A 149:615–620. https://doi.org/10.1016/j.saa.2015.04.109
28. Chang H, Lv J, Zhang H, Zhang B, Wei W, Qiao Y (2017) Photoresponsive colorimetric immunoassay based on chitosan modified AgI/TiO$_2$ heterojunction for highly sensitive chloramphenicol detection. Biosens Bioelectron 87:579–586. https://doi.org/10.1016/j.bios.2016.09.002
29. Karaseva NA, Ermolaeva TN (2012) A piezoelectric immunosensor for chloramphenicol detection in food. Talanta 93:44–48. https://doi.org/10.1016/j.talanta.2011.12.047
30. Bai X, Qin C, Huang X (2016) Voltammetric determination of chloramphenicol using a carbon fiber microelectrode modified with Fe$_3$O$_4$ nanoparticles. Microchim Acta 183(11):2973–2981. https://doi.org/10.1007/s00604-016-1945-x

31. Wang A, Zhang L, Fang Y (1999) Determination and separation of chloramphenicol and its hydrolysate in eye-drops by capillary zone electrophoresis with amperometric detection. Anal Chim Acta 394(2):309–316. https://doi.org/10.1016/S0003-2670(99)00314-1
32. Pilehvar S, Mehta J, Dardenne F, Robbens J, Blust R, De Wael K (2012) Aptasensing of chloramphenicol in the presence of its analogues: reaching the maximum residue limit. Anal Chem 84(15): 6753–6758. https://doi.org/10.1021/ac3012522
33. Feng YX, Bing LN, Qun LH (2012) Post-chemiluminescence determination of chloramphenicol based on luminol-potassium periodate system. Luminescence 27(3):217–222. https://doi.org/10.1002/bio.1335
34. Yan L, Luo C, Cheng W, Mao W, Zhang D, Ding S (2012) A simple and sensitive electrochemical aptasensor for determination of chloramphenicol in honey based on target-induced strand release. J Electroanal Chem 687:89–94. https://doi.org/10.1016/j.jelechem.2012.10.016
35. Wang Y, Bian F, Qin X, Wang Q (2018) Visible light photoelectrochemical aptasensor for chloramphenicol by using a TiO_2 nanorod array sensitized with Eu(III)-doped CdS quantum dots. Microchim Acta 185(3):161. https://doi.org/10.1007/s00604-018-2711-z